symmetry

MDPI

Article

On the Network Index of MAS with Layered Lattice-like Structures of Multiple Vertex-Related Parameters

Da Huang [1,*], Jibin Yang [2], Zhiyong Yu [3] and Cheng Hu [3]

[1] School of Mathematics and Physics, Xinjiang Institute of Engineering, Urumqi 830023, China
[2] School of Mathematics and Data Science, Changji University, Changji 831100, China; yjb24959@163.com
[3] School of Mathematics and System Science, Xinjiang University, Urumqi 830017, China; yzygsts@xju.edu.cn (Z.Y.); hucheng@xju.edu.cn (C.H.)
* Correspondence: hd@xjie.edu.cn or xiaoda86op@163.com

Abstract: In this article, a robust index named first-order network coherence (FONC) for the multi-agent systems (MASs) with layered lattice-like structure is studied via the angle of the graph spectra theory. The union operation of graphs is utilized to construct two pairs of non-isomorphic layered lattice-like structures, and the expression of the index is acquired by the approach of Laplacian spectra, then the corresponding asymptotic results are obtained. It is found that when the cardinality of the node sets of coronary substructures with better connectedness tends to infinity, the FONC of the whole network will have the same asymptotic behavior with the central lattice-like structure in the considered classic graph frameworks. The indices of the networks were simulated to illustrate the the asymptotic results, as described in the last section.

Keywords: multi-agent system (MAS); consensus; graph operation; fan graph; Laplacian spectra

Citation: Huang, D.; Yang, J.; Yu, Z.; Hu, C. On the Network Index of MAS with Layered Lattice-like Structures of Multiple Vertex-Related Parameters. *Symmetry* **2024**, *16*, 243. https://doi.org/10.3390/sym16020243

Academic Editors: Theodore E. Simos and Aviv Gibali

Received: 25 January 2024
Revised: 13 February 2024
Accepted: 14 February 2024
Published: 16 February 2024

1. Introduction

Multi-agent systems (MASs) are widely studied in many kinds of real applied networks, such as robotic systems [1], traffic networks [2], and unmanned aerial vehicle (UAV) networks. As an important MAS-related problem, the consensus problem refers to vertices achieving a identical physical status in some dynamical networked systems.

The consensus problem has been widely studied in many valuable works through various research factors [3–19] including but not limited to the system order (first or second order [3–6]), graphical types (digraph [5] or undirected graph, fixed or switching topology), continuity of the system (continuous or discrete time [7]), and type of control protocols (adaptive control [8–11], intermittent control [9,11], impulsive control [11], or event-trigger control [11,13]).

In the synchronization or consensus problems, the means of connecting the coordination-related systems are always characterized by a topological structure [3–28], and the method of algebraic graph theory is applied [3,14–25]. The enlightening research of Reference [14] has given the system robustness from the Laplacian eigenvalues of several classic graphs.

The robust performance of the consensus networks can be characterized by network coherence [15,16]. The articles mention that the performance index can be characterized by mathematical expressions related to Laplacian eigenvalues. Reference [19] shows the changing relationship between the consensus-related index in symmetric and asymmetric trees and the number of leader nodes. Reference [20] obtains the recursive expressions of Laplacian eigenvalues and further derives the exact results of first- and second-order coherence.

During the past decades, the multi-layer network [29] has become a leading topic as a result of its expansive real-world applications. Many networks have layered structures [21–24,26,29,30]; however, in the research branch of coordination problems, articles that incorporate the theory on Laplacian eigenvalues for consensus index of multi-layered networks are relatively rare. The fan graph is a classic structure since it can be viewed as

adhering connections between the leaves of the star graph, and the star graph is a classic structure of sensor networks. The wheel graph can be interpreted to add a new node and link it to each node of a cycle. There exist lots of wheel structure related research in application problems and graph theory research problems.

Considering these classical structures, and inspired by enlightening articles, this paper considers four sorts of MASs with layered lattice-like structures composed by graph operations.

The novelties of this article are listed as follows:

I. The union of graphs is introduced to form the novel non-isomorphic layered lattice-like structures for the network, and the notion that the peripheral coronary substructure need not be a single classic graph but can be a union of several subgraphs is proposed.
II. The graph spectra theory combined with the double integral approach are applied to derive the asymptotic results.
III. We find that when the cardinality of the node sets of coronary substructures with better connectedness tends to infinity, the FONC of the whole network will have approximately asymptotic behavior with the central lattice-like structure in the considered graph frameworks.

Section 2 gives the notations in basic graph theory, and the relation for the Laplacian spectra and index are interpreted. In Section 3, according to the theory of graph spectra, the topologies of the networks are proposed, and the asymptotic results are given. The simulation examples are analyzed and compared in Section 4.

2. Preliminaries

2.1. Basic Notations in Graph Theory

The empty graph with h vertices is denoted by $\mathfrak{E}_h$. Let G be an undirected graph with the vertex set $\mathcal{V}(G) = \{v_1, v_2, \ldots, v_N\}$, and its edge set $\mathcal{E}(G) = \{(v_i, v_j)|i, j = 1, 2, \ldots, N; i \neq j\}$. For any $v_i, v_j \in \mathcal{V}(G)$, (v_i, v_j) is in $\mathcal{E}(G)$ if and only if v_i is adjacent to v_j. $\mathcal{A}(G) = [a_{ij}]_N$ is the adjacency matrix, where the elements a_{ij} satisfy $a_{ij} = a_{ji}$. In this article, it is supposed that $a_{ij} = 1$, if $(v_i, v_j) \in \mathcal{E}(G)$; otherwise, $a_{ij} = 0$. The Laplacian matrix is defined as $\mathfrak{L}(G) = \mathcal{D}(G) - \mathcal{A}(G)$, where $\mathcal{D}(G) = diag(d_1, d_2, \ldots, d_N)$ with $d_i = \sum_{j \neq i} a_{ij}$. The Laplacian spectrum of G is defined as $SL(G) = \begin{pmatrix} \rho_1(G) & \rho_2(G) & \ldots & \rho_r(G) \\ l_1 & l_2 & \ldots & l_r \end{pmatrix}$, where $\rho_1(G) < \rho_2(G) < \cdots < \rho_r(G)$ are the eigenvalues of $\mathfrak{L}(G)$, and $l_1, l_2, \ldots, l_r$ are the multiplicities of the eigenvalues [31].

To describe the layered lattice-like structures, the corona operation of two graphs is denoted by '$\circ$' [32–35], the Cartesian product by '$\square$' [36–38], and the union operation by '$\cup$' [31,36].

Lemma 1 ([31,33]). *If two graphs G_1 and G_2 have c and d vertices, respectively, then the Laplacian eigenvalues of $G_1 \square G_2$ are given as: $\kappa_i(G_1) + \kappa_j(G_2)$, $(i = 1, 2 \ldots, c;\ j = 1, 2, \ldots, d)$, where $\kappa_i(G_1)$ and $\kappa_j(G_2)$ are the L-eigenvalues of G_1 and G_2.*

2.2. The Mathematical Description for FONC

Referring to References [14–20], the first-order MASs with additive noise is described by

$$\dot{x}(t) = -\mathfrak{L}x(t) + \phi(t), \tag{1}$$

where $x(t) \in R^N$, $\mathfrak{L}$ is the Laplacian matrix, and $\phi(t) \in R^N$ is a vector of uncorrelated noise.

Referring to [15,16], the first-order network coherence (FONC) is defined as:

$$\mathcal{H} = \lim_{t \to \infty} \frac{1}{N} \sum_{i=1}^{N} \mathrm{Var}\left\{ x_i(t) - \frac{1}{N} \sum_{j=1}^{N} x_j(t) \right\}.$$

The FONC can be given by the Laplacian eigenvalues, i.e.,

$$\mathcal{H} = \frac{1}{2N} \sum_{i=2}^{N} \frac{1}{\rho_i}. \tag{2}$$

This expression shares similarities with the Kirchhoff index [33,39–41] and other network indices [42].

3. Main Results

The system topologies in this research are interpreted as a class of layered lattice-like structure consisting of several classic subgraph copies, and they will be characterized in Sections 3.1–3.4.

3.1. The FONC for Network $\mathfrak{F}_1$

In this subsection, a sort of layered lattice-like topology based on the wheel and fan graph is considered. As shown in Figure 1, the structure can be seen as a wheel graph in each layer, and the links among each layer are designed to form the fan graph. By the graph operation, the structure is defined by $F_1(p,q,a,b) := (W_p \square F_q) \circ (K_a \cup \mathfrak{E}_b)$ and abbreviated as $\mathcal{F}_1$, where p,q denotes the cardinality of the node sets of the wheel and fan substructure; a denotes the number of vertices of the complete subgraph in the peripheral coronary substructure; b denotes the number of vertices of degree one in one corona copy, i.e., $(K_a \cup \mathfrak{E}_b)$ (see Figure 2; the example $P_3 \circ (K_4 \cup E_3)$ is to explain the peripheral coronary structure); and the corresponding network with disturbance is denoted as $\mathfrak{F}_1$.

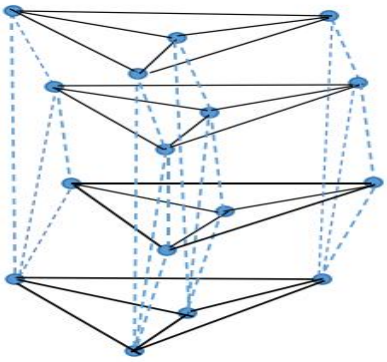

Figure 1. A graph example of $W_p \square F_q$, $p = 4, q = 4$.

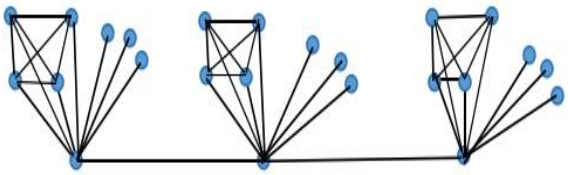

Figure 2. An example of the coronary substructure: $P_3 \circ (K_4 \cup E_3)$.

Since $SL(K_n) = \begin{pmatrix} 0 & n \\ 1 & n-1 \end{pmatrix}$,

$SL(W_p) = \begin{pmatrix} 0 & p & 1+4sin^2(\frac{i\pi}{p-1}) \\ 1 & 1 & 1 \end{pmatrix}$, where $i = 1,2,\ldots,p-2$.

$SL(F_q) = \begin{pmatrix} 0 & q & 1+4sin^2(\frac{j\pi}{2(q-1)}) \\ 1 & 1 & 1 \end{pmatrix}$, where $j = 1,2,\ldots,p-2$.

Therefore, according to Lemma 1 (on the L-spectrum of the Cartesian product of two graphs [31,33]), $SL(W_p \square F_q)$ has the following characterization:

(1). $0, q, p, p+q \in SL(W_p \square F_q)$ with multiplicity 1;
(2). $1+4sin^2(\frac{j\pi}{2(q-1)}), p+1+4sin^2(\frac{j\pi}{2(q-1)}) \in SL(W_p \square F_q)$ with multiplicity 1, where $j = 1, 2 \ldots, q-2$.
(3). $1+4sin^2(\frac{i\pi}{(p-1)}), q+1+4sin^2(\frac{i\pi}{(p-1)}) \in SL(W_p \square F_q)$ with multiplicity 1, where $i = 1, 2, \ldots, p-2$.
(4). $2+4sin^2(\frac{i\pi}{(p-1)})+4sin^2(\frac{j\pi}{2(q-1)}) \in SL(W_p \square F_q)$ with multiplicity 1, where $i = 1, 2, \ldots, p-2$, $j = 1, 2 \ldots, q-2$.

The L-spectrum of the subgraph $(K_a \cup \mathfrak{E}_b)$ can be described as:

$$SL(K_a \cup \mathfrak{E}_b) = \begin{pmatrix} 0 & a \\ b+1 & a-1 \end{pmatrix};$$

Then, according to the theorem on the corona operation [32,33], the characterization of $SL(\mathcal{F}_1)$ can be listed as follows:

(1). 0 and $a+b+1 \in SL(\mathcal{F}_1)$ with multiplicity 1;
(2). $\frac{(q+a+b+1)\pm\sqrt{(q+a+b+1)^2-4q}}{2} \in SL(\mathcal{F}_1)$ with multiplicity 1; $\frac{(p+a+b+1)\pm\sqrt{(p+a+b+1)^2-4p}}{2} \in SL(\mathcal{F}_1)$ with multiplicity 1; $\frac{(p+q+a+b+1)\pm\sqrt{(p+q+a+b+1)^2-4(p+q)}}{2} \in SL(\mathcal{F}_1)$ with multiplicity 1.
(3). $\frac{(2+4sin^2(\frac{j\pi}{2(q-1)})+a+b)\pm\sqrt{(2+4sin^2(\frac{j\pi}{2(q-1)})+a+b)^2-4(1+4sin^2(\frac{j\pi}{2(q-1)}))}}{2} \in SL(\mathcal{F}_1)$ with multiplicity 1, where $j = 1, 2, \ldots, q-2$.
(4). $\frac{(p+2+4sin^2(\frac{j\pi}{2(q-1)})+a+b)\pm\sqrt{(p+2+4sin^2(\frac{j\pi}{2(q-1)})+a+b)^2-4(p+1+4sin^2(\frac{j\pi}{2(q-1)}))}}{2} \in SL(\mathcal{F}_1)$ with multiplicity 1, where $j = 1, 2, \ldots, q-2$.
(5). $\frac{(2+4sin^2(\frac{i\pi}{p-1})+a+b)\pm\sqrt{(2+4sin^2(\frac{i\pi}{p-1})+a+b)^2-4(1+4sin^2(\frac{i\pi}{p-1}))}}{2} \in SL(\mathcal{F}_1)$ with multiplicity 1, where $i = 1, 2, \ldots, p-2$.
(6). $\frac{(q+2+4sin^2(\frac{i\pi}{p-1})+a+b)\pm\sqrt{(q+2+4sin^2(\frac{i\pi}{p-1})+a+b)^2-4(q+1+4sin^2(\frac{i\pi}{p-1}))}}{2} \in SL(\mathcal{F}_1)$ with multiplicity 1, where $i = 1, 2, \ldots, p-2$.
(7). $\frac{(3+4sin^2(\frac{i\pi}{p-1})+4sin^2(\frac{j\pi}{2(q-1)})+a+b)\pm\sqrt{(3+4sin^2(\frac{i\pi}{p-1})+4sin^2(\frac{j\pi}{2(q-1)})+a+b)^2-4(2+4sin^2(\frac{i\pi}{p-1})+4sin^2(\frac{j\pi}{2(q-1)}))}}{2}$ $\in SL(\mathcal{F}_1)$ with multiplicity 1, where $i = 1, 2, \ldots, p-2$; $j = 1, 2, \ldots, q-2$.
(8). $1 \in SL(\mathcal{F}_1)$ repeated bpq times; $a+1 \in SL(\mathcal{F}_1)$ repeated $pq(a-1)$ times.

Therefore, the FONC of $\mathfrak{F}_1$ is:

$$\begin{aligned} H(\mathfrak{F}_1) =& \frac{1}{2N}\sum_{k=2}^{N}\frac{1}{\rho_k} \\ =& \frac{1}{2(pq+pq(a+b))}\Bigg(\frac{1}{a+b+1}+\frac{q+a+b+1}{q}+\sum_{j=1}^{q-2}\frac{2+4sin^2(\frac{j\pi}{2(q-1)})+a+b}{1+4sin^2(\frac{j\pi}{2(q-1)})} \\ &+\frac{p+a+b+1}{p}+\frac{p+q+a+b+1}{p+q}+\sum_{j=1}^{q-2}\frac{p+2+4sin^2(\frac{j\pi}{2(q-1)})+a+b}{p+1+4sin^2(\frac{j\pi}{2(q-1)})} \\ &+\sum_{i=1}^{p-2}\frac{2+4sin^2(\frac{i\pi}{(p-1)})+a+b}{1+4sin^2(\frac{i\pi}{(p-1)})}+\sum_{i=1}^{p-2}\frac{q+2+4sin^2(\frac{i\pi}{(p-1)})+a+b}{q+1+4sin^2(\frac{i\pi}{(p-1)})} \\ &+\sum_{j=1}^{q-2}\sum_{i=1}^{p-2}\frac{3+4sin^2(\frac{i\pi}{(p-1)})+4sin^2(\frac{j\pi}{(2(q-1))})+a+b}{2+4sin^2(\frac{i\pi}{(p-1)})+4sin^2(\frac{j\pi}{2(q-1)})}+bpq+\frac{pq(a-1)}{a+1}\Bigg). \end{aligned}$$

Therefore, we have

$$\begin{aligned}\lim_{p,q\to\infty} H(\mathfrak{F}_1) =& \frac{1}{2(1+a+b)} + \frac{1}{2}\int_0^1\int_0^1 \frac{1}{2+4sin^2(\pi x)+4sin^2(\frac{\pi y}{2})}dxdy \\ &+ \frac{b}{2(1+a+b)} + \frac{a-1}{2(1+a+b)(a+1)} \\ =& \frac{2a+ab+b}{2(1+a+b)(a+1)} + 0.096.\end{aligned}$$

It can be seen that if the cardinality of the coronary complete substructure, i.e., a, is large enough, the performance index will tend to 0.096, and if b tends to infinity, then the asymptotic index will be 0.596.

3.2. The Performance Index for $\mathfrak{F}_2$

In this subsection, a class of lattice-like star-fan composed network is designed. The vertices in the peripheral subgraph are required to be disconnected with other layers. The layered lattice-like structure is defined by $F_2(p,q,a,b) := (W_p \square F_q) \circ (P_a \cup \mathfrak{E}_b)$ and abbreviated as $\mathcal{F}_2$, where p, q denote the number of vertices in the wheel and fan graph of the lattice-like central structure (see Figure 1), and the corresponding noisy network is denoted as $\mathfrak{F}_2$. Figure 3 gives an example to show the partial coronary substructure, i.e., P_a. It is designed to form a fan graph copy during the graph operation, and the other part of the peripheral substructure is designed to be a star graph copy.

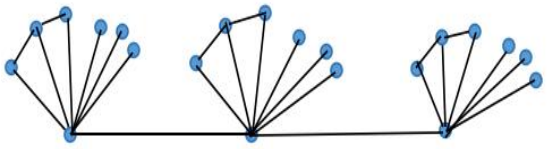

Figure 3. An example of the coronary substructure: $P_3 \circ (P_3 \cup E_3)$.

Since $SL(P_a) = (0, 4sin^2(\frac{k\pi}{2a}))$, $k = 1, 2, \ldots, a-1$,

$SL(P_a \cup \mathfrak{E}_b) = \begin{pmatrix} 0 & 4sin^2(\frac{m\pi}{2a}) \\ b+1 & a-1 \end{pmatrix}$, where $m = 1, 2, \ldots, a-1$.

According to lemmas on the coronary graph operation [32,33], the L-spectrum $SL(\mathcal{F}_2)$ has the characterization as follows:

(1). 0 and $a+b+1 \in SL(\mathcal{F}_2)$ with multiplicity 1;

(2). $\frac{(q+a+b+1)\pm\sqrt{(q+a+b+1)^2-4q}}{2} \in SL(\mathcal{F}_2)$ with multiplicity 1; $\frac{(p+a+b+1)\pm\sqrt{(p+a+b+1)^2-4p}}{2} \in SL(\mathcal{F}_2)$ with multiplicity 1; $\frac{(p+q+a+b+1)\pm\sqrt{(p+q+a+b+1)^2-4(p+q)}}{2} \in SL(\mathcal{F}_2)$ with multiplicity 1.

(3). $\frac{(2+4sin^2(\frac{j\pi}{2(q-1)})+a+b)\pm\sqrt{(2+4sin^2(\frac{j\pi}{2(q-1)})+a+b)^2-4(1+4sin^2(\frac{j\pi}{2(q-1)}))}}{2} \in SL(\mathcal{F}_2)$ with multiplicity 1, where $j = 1, 2, \ldots, q-2$.

(4). $\frac{(p+2+4sin^2(\frac{j\pi}{2(q-1)})+a+b)\pm\sqrt{(p+2+4sin^2(\frac{j\pi}{2(q-1)})+a+b)^2-4(p+1+4sin^2(\frac{j\pi}{2(q-1)}))}}{2} \in SL(\mathcal{F}_2)$ with multiplicity 1, where $j = 1, 2, \ldots, q-2$.

(5). $\frac{(2+4sin^2(\frac{i\pi}{p-1})+a+b)\pm\sqrt{(2+4sin^2(\frac{i\pi}{p-1})+a+b)^2-4(1+4sin^2(\frac{i\pi}{p-1}))}}{2} \in SL(\mathcal{F}_2)$ with multiplicity 1, where $i = 1, 2, \ldots, p-2$.

(6). $\frac{(q+2+4sin^2(\frac{i\pi}{p-1})+a+b)\pm\sqrt{(q+2+4sin^2(\frac{i\pi}{p-1})+a+b)^2-4(q+1+4sin^2(\frac{i\pi}{p-1}))}}{2} \in SL(\mathcal{F}_2)$ with multiplicity 1, where $i = 1, 2, \ldots, p-2$.

(7). $\frac{(3+4sin^2(\frac{i\pi}{p-1})+4sin^2(\frac{j\pi}{2(q-1)})+a+b)\pm\sqrt{(3+4sin^2(\frac{i\pi}{p-1})+4sin^2(\frac{j\pi}{2(q-1)})+a+b)^2-4(2+4sin^2(\frac{i\pi}{p-1})+4sin^2(\frac{j\pi}{2(q-1)}))}}{2}$ $\in SL(\mathcal{F}_2)$ with multiplicity 1, where $i = 1, 2, \ldots, p-2$; $j = 1, 2, \ldots, q-2$.

(8). $1 \in SL(\mathcal{F}_2)$ repeated bpq times; $4sin^2(\frac{m\pi}{2a}) + 1 \in SL(\mathcal{F}_2)$ repeated pq times, where $m = 1, 2, \ldots, a-1$.

It can be seen that the only difference of L-spectrum between $\mathfrak{F}_1$ and $\mathfrak{F}_2$ is the item (8) above; that is, $4sin^2(\frac{m\pi}{2a})+1 \in SL(\mathcal{F}_2)$ repeated pq times.

Therefore, similarly, the FONC of $\mathfrak{F}_2$ can be obtained, and it is omitted here. When $p, q \to \infty$, the asymptotic difference of FONC between $\mathfrak{F}_2$ and $\mathfrak{F}_1$, denoted by $\nabla\mathfrak{F}_{12}$, can be obtained:

$$\nabla\mathfrak{F}_{12} \to \frac{1}{2(a+b+1)}\left[\sum_{m=1}^{a-1}\frac{1}{4sin^2(\frac{m\pi}{2a})+1}-\frac{a-1}{a+1}\right]. \tag{3}$$

Hence, it can be determined that the asymptotic difference tends to $\frac{\sqrt{5}}{10}$ as a tends to infinity, and the asymptotic value of $H(\mathfrak{F}_2)$ is larger than that of $H(\mathfrak{F}_1)$; when b is large enough, they have the same asymptotic index, and it can be interpreted as the asymptotic result of the difference above being closed when b tends to infinity.

Remark 1. *In fact, if the layered lattice-like structure is changed to* $(F_p \square F_q) \circ (P_a \cup \mathfrak{E}_b)$*, then the same asymptotic results with the above section can be obtained. These results are omitted here.*

Remark 2. *The construction design of this coronary structure implies that the peripheral substructure of each layer may not simply be a star or fan graph but may be a graph composed of several different classic subgraphs. The lattice-like structure in the middle can be interpreted as consisting of the hub nodes with the highest degree.*

3.3. The Performance Index for $\mathfrak{F}_3$

The network structure in this subsection is described as follows. From a vertical view, the counterpart nodes with a higher degree of different layers are designed to form the fan graph, and the coronary substructure is a balanced complete k-partite graph. The graph is characterized by $F_3(p,q,a,m) := (W_p \square F_q) \circ (K(a,m))$ and abbreviated as $\mathcal{F}_3$, where the definition of p, q is the same as that of Section 3.2, and a, m means the multipartite substructure being acted on has a partition of vertex set and each part has m vertices. The related noisy network is denoted by $\mathfrak{F}_3$. Figure 4 gives an example of the coronary substructures placed on each node of P_3.

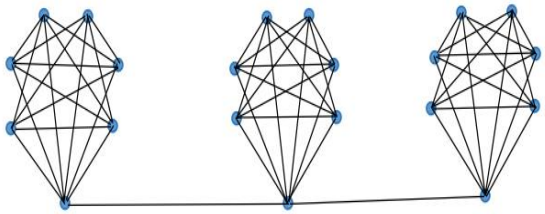

Figure 4. An example of the coronary substructure: $P_3 \circ (K(2,3))$.

The L-spectrum of $K(a,m)$ can be characterized by:

$$SL(K(a,m)) = \begin{pmatrix} 0 & am & (a-1)m \\ 1 & a-1 & am-a \end{pmatrix}$$

Thus, the Laplacian spectrum of $\mathcal{F}_3$ can be described as follows:

(1). 0 and $am+1 \in SL(\mathcal{F}_3)$ with multiplicity 1;

(2). $\frac{(q+am+1)\pm\sqrt{(q+a+b+1)^2-4q}}{2} \in SL(\mathcal{F}_3)$ with multiplicity 1; $\frac{(p+am+1)\pm\sqrt{(p+am+1)^2-4p}}{2} \in SL(\mathcal{F}_3)$ with multiplicity 1; $\frac{(p+q+am+1)\pm\sqrt{(p+q+am+1)^2-4(p+q)}}{2} \in SL(\mathcal{F}_3)$ with multiplicity 1.

(3). $\frac{(2+4sin^2(\frac{j\pi}{2(q-1)})+am)\pm\sqrt{(2+4sin^2(\frac{j\pi}{2(q-1)})+am)^2-4(1+4sin^2(\frac{j\pi}{2(q-1)}))}}{2} \in SL(\mathcal{F}_3)$ with multiplicity 1, where $j = 1, 2, \ldots, q-2$.

(4). $\frac{(p+2+4sin^2(\frac{j\pi}{2(q-1)})+am)\pm\sqrt{(p+2+4sin^2(\frac{j\pi}{2(q-1)})+am)^2-4(p+1+4sin^2(\frac{j\pi}{2(q-1)}))}}{2} \in SL(\mathcal{F}_3)$ with multiplicity 1, where $j = 1, 2, \ldots, q-2$.

(5). $\frac{(2+4sin^2(\frac{i\pi}{p-1})+am)\pm\sqrt{(2+4sin^2(\frac{i\pi}{p-1})+am)^2-4(1+4sin^2(\frac{i\pi}{p-1}))}}{2} \in SL(\mathcal{F}_3)$ with multiplicity 1, where $i = 1, 2, \ldots, p-2$.

(6). $\frac{(q+2+4sin^2(\frac{i\pi}{p-1})+am)\pm\sqrt{(q+2+4sin^2(\frac{i\pi}{p-1})+am)^2-4(q+1+4sin^2(\frac{i\pi}{p-1}))}}{2} \in SL(\mathcal{F}_3)$ with multiplicity 1, where $i = 1, 2, \ldots, p-2$.

(7). $\frac{(3+4sin^2(\frac{i\pi}{p-1})+4sin^2(\frac{j\pi}{2(q-1)})+am)\pm\sqrt{(3+4sin^2(\frac{i\pi}{p-1})+4sin^2(\frac{j\pi}{2(q-1)})+am)^2-4(2+4sin^2(\frac{i\pi}{p-1})+4sin^2(\frac{j\pi}{2(q-1)}))}}{2}$ $\in SL(\mathcal{F}_3)$ with multiplicity 1, where $i = 1, 2, \ldots, p-2$; $j = 1, 2, \ldots, q-2$.

(8). $am+1 \in SL(\mathcal{F}_3)$ repeated $(a-1)pq$ times; $(a-1)m+1 \in SL(\mathcal{F}_3)$ repeated $(am-a)pq$ times.

Hence, the FONC of $\mathfrak{F}_3$ can be derived as:

$$\begin{aligned}
H(\mathfrak{F}_3) =& \frac{1}{2N}\sum_{k=2}^{N}\frac{1}{\rho_k} \\
=& \frac{1}{2(pq+pqam)}\Bigg(\frac{1}{am+1}+\frac{q+am+1}{q}+\sum_{j=1}^{q-2}\frac{2+4sin^2(\frac{j\pi}{2(q-1)})+am}{1+4sin^2(\frac{j\pi}{2(q-1)})} \\
&+\frac{p+am+1}{p}+\frac{p+q+am+1}{p+q}+\sum_{j=1}^{q-2}\frac{p+2+4sin^2(\frac{j\pi}{2(q-1)})+am}{p+1+4sin^2(\frac{j\pi}{2(q-1)})} \\
&+\sum_{i=1}^{p-2}\frac{2+4sin^2(\frac{i\pi}{(p-1)})+am}{1+4sin^2(\frac{i\pi}{(p-1)})}+\sum_{i=1}^{p-2}\frac{q+2+4sin^2(\frac{i\pi}{(p-1)})+am}{q+1+4sin^2(\frac{i\pi}{(p-1)})} \\
&+\sum_{j=1}^{q-2}\sum_{i=1}^{p-2}\frac{3+4sin^2(\frac{i\pi}{(p-1)})+4sin^2(\frac{j\pi}{(2(q-1))})+am}{2+4sin^2(\frac{i\pi}{(p-1)})+4sin^2(\frac{j\pi}{2(q-1)})}+\frac{1}{am+1}(a-1)pq \\
&+\frac{1}{(a-1)m+1}(am-a)pq\Bigg).
\end{aligned}$$

Therefore, we have

$$\begin{aligned}
\lim_{p,q\to\infty}H(\mathfrak{F}_3) =& \frac{1}{2(1+am)}+\frac{1}{2}\int_0^1\int_0^1\frac{1}{2+4sin^2(\pi x)+4sin^2(\frac{\pi y}{2})}dxdy \\
&+\frac{a-1}{2(1+am)^2}+\frac{am-a}{2(1+am)(am-m+1)} \\
=& \frac{am+a}{2(1+am)^2}+\frac{am-a}{2(1+am)(am-m+1)}+0.096.
\end{aligned}$$

We can see that if the parameter a or m is large enough, the coherence index will approximate to 0.096.

Remark 3. *When p, q and m are fixed, and if the parameter $a \to +\infty$ is considered, we can find that the asymptotic result of $H(\mathfrak{F}_3)$ is irrelevant to m, and we have $H(\mathfrak{F}_3) \to \frac{1}{2pq^2}+\frac{1}{2p^2q}+\frac{1}{2pq(p+q)}+\frac{1}{2pq}\Big[\sum_{j=1}^{q-2}\frac{1}{1+4sin^2(\frac{j\pi}{2(q-1)})}+\sum_{j=1}^{p-2}\frac{1}{1+4sin^2(\frac{j\pi}{(p-1)})}+\sum_{j=1}^{q-2}\frac{1}{p+1+4sin^2(\frac{j\pi}{2(q-1)})}+\sum_{j=1}^{p-2}\frac{1}{q+1+4sin^2(\frac{j\pi}{(p-1)})}+\sum_{j=1}^{q-2}\sum_{i=1}^{p-2}\frac{1}{2+4sin^2(\frac{i\pi}{(p-1)})+4sin^2(\frac{j\pi}{2(q-1)})}\Big]$. Similarly, when m tends to infinity, the limitation is irrelevant to the parameter a, and we omit the result here.*

3.4. The Performance Index for $\mathfrak{F}_4$

In this subsection, a lattice-like structure with a sort of multi-fan composed graph as the coronary peripheral structure (see Figure 5) is considered. Intuitively speaking, the structure's formation can be seen as adhering copied multi-paths to each nodes of the lattice-like structure. Thus, $\mathcal{F}_4 := (W_p \square F_q) \circ (\cup_a P_m)$.

Figure 5. An example of the coronary substructure for $\mathcal{F}_4$: $P_3 \circ (\cup_3(P_3))$.

The L-spectrum of $SL(\cup_a P_m) = \begin{pmatrix} 0 & 4sin^2\frac{k\pi}{2m} \\ a & a \end{pmatrix}$, where $k = 1, 2, \ldots, m-1$.

Hence, the L-spectrum of $\mathcal{F}_4$ has the following description:

The conclusions (1)–(7) are the same as those of $SL(\mathcal{F}_3)$, and the item (8) has changed into $1 \in SL(\mathcal{F}_4)$ repeated $(a-1)pq$ times and $4sin^2\frac{k\pi}{2m} + 1 \in SL(\mathcal{F}_4)$ with multiplicity apq, where $k = 1, 2, \ldots m-1$.

Therefore, the FONC of $\mathfrak{F}_4$ is:

$$\begin{aligned} H(\mathfrak{F}_4) =& \frac{1}{2N}\sum_{k=2}^{N}\frac{1}{\rho_k} \\ =& \frac{1}{2(pq+pqam)}\Bigg(\frac{1}{am+1} + \frac{q+am+1}{q} + \sum_{j=1}^{q-2}\frac{2+4sin^2(\frac{j\pi}{2(q-1)})+am}{1+4sin^2(\frac{j\pi}{2(q-1)})} \\ &+ \frac{p+am+1}{p} + \frac{p+q+am+1}{p+q} + \sum_{j=1}^{q-2}\frac{p+2+4sin^2(\frac{j\pi}{2(q-1)})+am}{p+1+4sin^2(\frac{j\pi}{2(q-1)})} \\ &+ \sum_{i=1}^{p-2}\frac{2+4sin^2(\frac{i\pi}{(p-1)})+am}{1+4sin^2(\frac{i\pi}{(p-1)})} + \sum_{i=1}^{p-2}\frac{q+2+4sin^2(\frac{i\pi}{(p-1)})+am}{q+1+4sin^2(\frac{i\pi}{(p-1)})} \\ &+ \sum_{j=1}^{q-2}\sum_{i=1}^{p-2}\frac{3+4sin^2(\frac{i\pi}{(p-1)})+4sin^2(\frac{j\pi}{(2(q-1))})+am}{2+4sin^2(\frac{i\pi}{(p-1)})+4sin^2(\frac{j\pi}{2(q-1)})} + (a-1)pq \\ &+ \sum_{k=1}^{m-1}\frac{1}{4sin^2\frac{k\pi}{2m}+1}apq\Bigg). \end{aligned}$$

Similar to the FONC of $\mathfrak{F}_3$, it can be derived that $H(\mathfrak{F}_4) \to \frac{a}{2(1+am)}(1+\sum_{k=1}^{m-1}\frac{1}{4sin^2\frac{k\pi}{2m}+1}) + 0.096$; thus, $H(\mathfrak{F}_4)$ tends to $\frac{\sqrt{5}}{5} + 0.096$ when the parameter m is large enough, and meanwhile the difference between the FONC of $\mathfrak{F}_3$ and $\mathfrak{F}_4$ is equal to $\frac{\sqrt{5}}{5}$, and we also find that whether a or m is large enough, $H(\mathfrak{F}_3) < H(\mathfrak{F}_4)$ holds.

Remark 4. *It is supposed that the coronary copy of* $\mathfrak{F}_3$ *and* $\mathfrak{F}_4$ *has the same cardinality of vertex sets of partition; only the connection structures within each partition and the links among all partition sets are different. Thus, the coronary linking structure of* $\mathfrak{F}_3$ *and* $\mathfrak{F}_4$*, which is located at the edge of the graph, has the same number of nodes; that is,* $|V(K(a,m))| = |V(\cup_a P_m)|$*. These two graph classes both have a parts, and each part has m vertices. One can see that when m is large enough (tends to infinity),* $H(\mathfrak{F}_4)$ *is 0.5 larger than* $H(\mathfrak{F}_3)$*, and when a tends to infinity,* $H(\mathfrak{F}_4)$ *is* $(1+\sum_{k=1}^{m-1}\frac{1}{4sin^2\frac{k\pi}{2m}+1})/2m$ *larger than* $H(\mathfrak{F}_3)$*.*

Remark 5. *The asymptotic results can be applied to analyze or improve the first-order network robustness. The layered lattice-like structure in this paper can be a reference for the research of layered weighted complex networks.*

4. Simulation

The coherence indices of the MASs with layered lattice-like graph are simulated and compared in this section.

As a simulation example for the changing relation of the coherence $H(\mathfrak{F}_1)$ and the other graph parameters, Figure 6 describes the change in coherence index with p and q when a and b are both fixed to 3.

When p and q both tend to infinity, $H(\mathfrak{F}_1) \to 0.417$ (see the point (46,43,0.4176)). This coincides with the calculation results of Section 3.1.

From Figure 6, one can also see that when one of p and q is fixed to a relatively small value, the change in p has a greater effect on the change in H. When p and q are both large enough, the robustness of the network is better than the case that one of p, q is relatively small.

Figure 7 describes the change surface of $H(\mathfrak{F}_2)$ with the parameters p and q when $a = b = 3$. It implies that the point (46,43,0.4355) is in accordance with the tendency $H(\mathfrak{F}_2) \to 0.4347$ as $p, q \to \infty$, and similar results to Figure 6 can be acquired. In Figure 8, the comparison of $H(\mathfrak{F}_1)$ and $H(\mathfrak{F}_2)$ with the change in p and q is given. From the point (49,49,0.4355) and (49,49,0.4176), we can see that the difference of the two function values is equal to 0.0179, which is consistent with the result (3) on page 6 . Figure 9 shows the variance of $H(\mathfrak{F}_3)$ with the change in a and m. Through Figure 9, we can see that when p, q are both relatively small, $H(\mathfrak{F}_3)$ is larger than that in the case where at least one of p, q is relatively large. The two pair of points (45, 100, 0.09928), (70, 100, 0.09921) and (100, 85, 0.09919), (100, 28, 0.09942) imply that when a or m tends to infinity, $H(F_3)$ will decrease monotonously to the constant 0.099, and the value is only relevant to p and q, which is consistent with Remark 3. Figure 10 shows the changing curve of $H(\mathfrak{F}_4)$ with a and m, $p = q = 3$. Compared with Figures 9 and 10, and combined with the result in Section 3.4, we find that when p, q are fixed to the same value for $H(\mathfrak{F}_3)$ and $H(\mathfrak{F}_4)$, the inequality $H(\mathfrak{F}_3) < H(\mathfrak{F}_4)$ always holds. When m , p, q are fixed, the coherence $H(\mathfrak{F}_4)$ will increase monotonously to a constant.

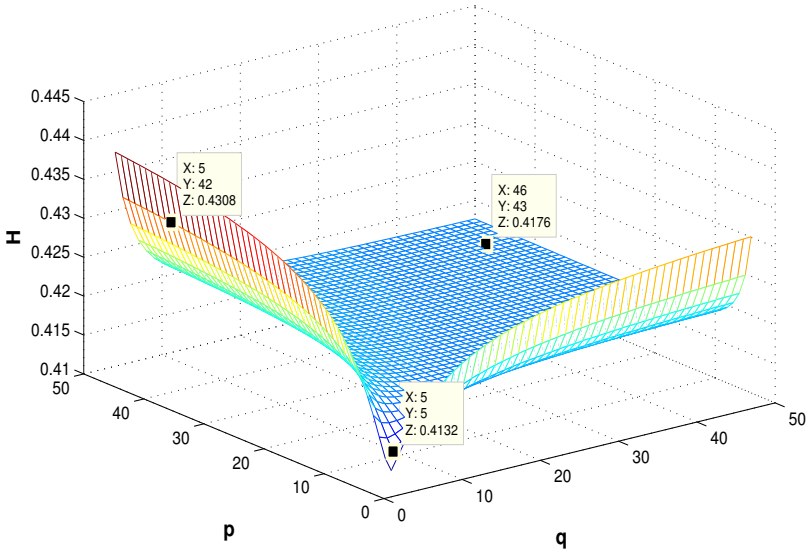

Figure 6. The change surface of $H(\mathfrak{F}_1)$ with p and q, $a = 3$, $b = 3$.

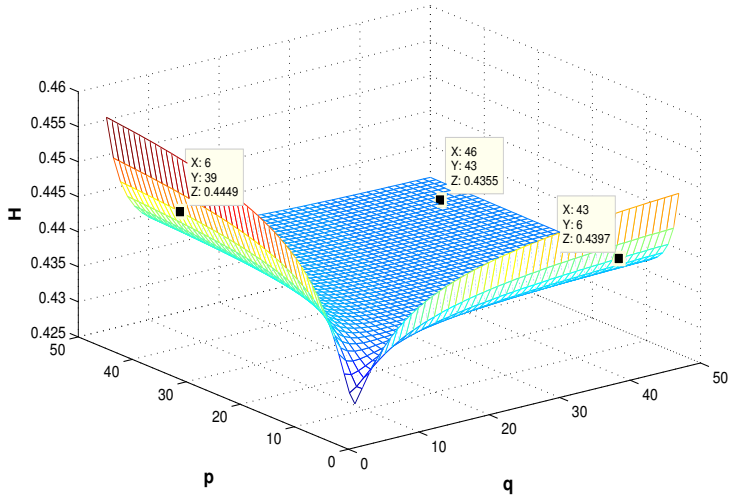

Figure 7. The change in $H(\mathfrak{F}_2)$ with p and q, $a = 3,\ b = 3$.

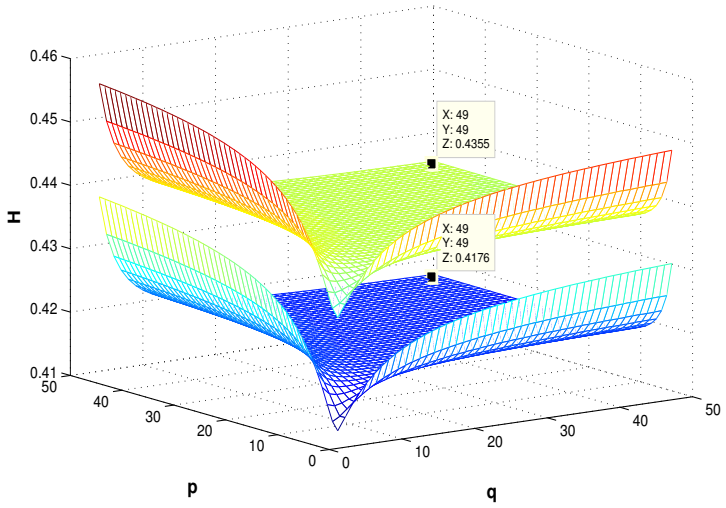

Figure 8. The comparison of $H(\mathfrak{F}_1)$ and $H(\mathfrak{F}_2)$ with the change in p and q, $a, b = 3$.

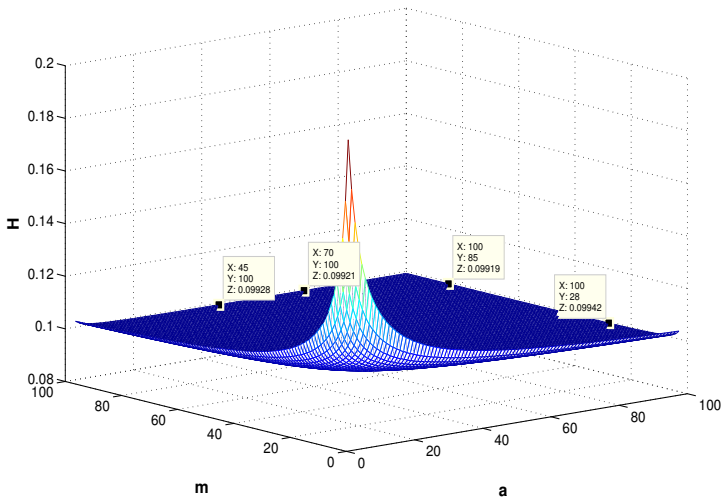

Figure 9. The variance of $H(\mathfrak{F}_3)$ with the change in a and m, where $p = q = 3$.

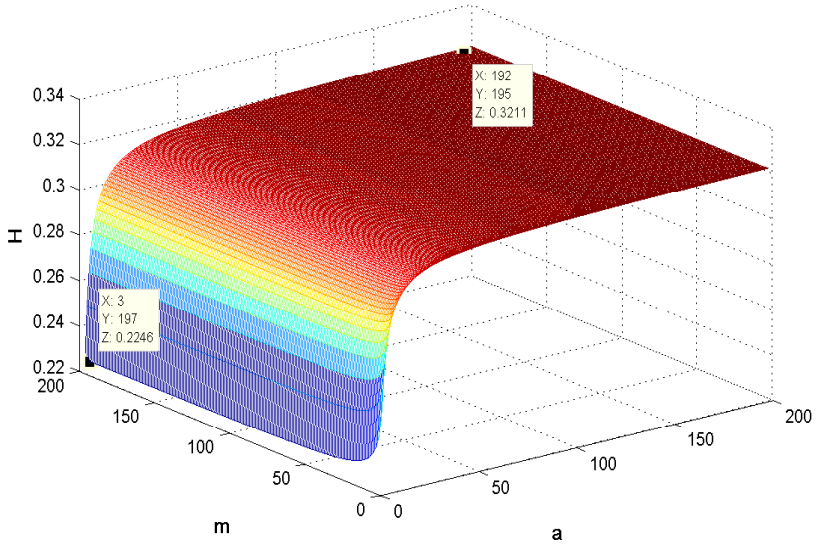

Figure 10. The variance of $H(\mathfrak{F}_4)$ with the change in a and m, where $p = q = 3$.

5. Conclusions

This article mainly studied the FONC of the layered noisy systems. To be specific, the methods of graph spectra were utilized to analyze the layered lattice-like graph, then the specific mathematical expressions for FONC were derived, and novel asymptotic results were acquired. We find that when the cardinality of the node sets of coronary substructures with better connectedness tends to infinity, the FONC of the whole network will have approximate asymptotic behavior with the central lattice-like structure in the considered classic graph frameworks.

Author Contributions: Methodology: D.H. and J.Y.; software: D.H. and J.Y.; validation: D.H., Z.Y. and C.H.; formal analysis: D.H. and J.Y.; writing—original draft preparation: D.H. and J.Y.; writing—review and editing: D.H., J.Y., Z.Y. and C.H.; supervision: Z.Y. and C.H.; project administration: D.H. All authors have read and agreed to the published version of the manuscript.

Funding: This work was supported by the Natural Science Foundation of Xinjiang (NSFXJ) (No. 2022D01A247), National Natural Science Foundation of People's Republic of China (NSFC) (Grant No. 12361110).

Data Availability Statement: Data are contained within the article.

Conflicts of Interest: The authors declare no conflict of interest

References

1. Piranda, B.; Lassabe, F.; Bourgeois, J. DisCo: A Multiagent 3D Coordinate System for Lattice Based Modular Self-Reconfigurable Robots. In Proceedings of the 2023 IEEE International Conference on Robotics and Automation (ICRA), London, UK, 29 May–2 June 2023 .
2. Akopov, A.S.; Beklaryan, L.A. Traffic Improvement in Manhattan Road Networks with the Use of Parallel Hybrid Biobjective Genetic Algorithm. *IEEE Access* **2024**, *12*, 19532–19552. [CrossRef]
3. Saber, O.; Murray, R. Consensus problems in Networks of Agents with Switching Topology and Time-Delays. *IEEE Trans. Autom. Control* **2004**, *49*, 1520–1533. [CrossRef]
4. Ren, W. On consensus algorithms for double-integrator dynamics. *IEEE Trans. Autom. Control* **2008**, *53*, 1503–1509. [CrossRef]
5. Yu, W.; Chen, G.; Cao, M.; Kurths, J. Second-order consensus for multiagent systems with directed topologies and nonlinear dynamics. *IEEE Trans. Syst. Man Cybern.-Part Cybern.* **2010**, *40*, 881–891.
6. Wen, G.; Duan, Z.; Yu, W.; Chen, G. Consensus of second-order multi-agent systems with delayed nonlinear dynamics and intermittent communications. *Int. J. Control* **2013**, *86*, 322–331. [CrossRef]
7. Xiao, F.; Wang, L. Consensus protocols for discrete-time multi-agent systems with time-varying delays. *Automatica* **2008**, *44*, 2577–2582. [CrossRef]
8. Yue, D.; Cao, J.; Li, Q.; Liu, Q. Neural-Network-Based Fully Distributed Adaptive Consensus for a Class of Uncertain Multiagent Systems. *IEEE Trans. Neural Netw. Learn. Syst.* **2021**, *32*, 2965–2977. [CrossRef]

9. Sun, J.; Guo, C.; Liu, L.; Shan, Q. Adaptive consensus control of second-order nonlinear multi-agent systems with event-dependent intermittent communications. *J. Frankl. Inst.* **2023**, *360*, 2289–2306. [CrossRef]
10. Yu, Z.; Jiang, H.; Hu, C.; Yu, J. Leader-following consensus of fractional-order multi-agent systems via adaptive pinning control. *Int. J. Control* **2015**, *88*, 1746–1756. [CrossRef]
11. Zhang, Y.; Wen, G.; Rahmani, A.; Peng, Z.; Hu, W. Cluster consensus of multi-agent systems with general linear and nonlinear dynamics via intermittent adaptive pinning control. *Trans. Inst. Meas. Control* **2021**, *43*, 1337–1346. [CrossRef]
12. Tan, X.; Cao, J.; Li, X. Consensus of Leader-Following Multiagent Systems: A Distributed Event-Triggered Impulsive Control Strategy. *IEEE Trans. Cybern.* **2019**, *49*, 792–801. [CrossRef]
13. Li, X.; Yu, Z.; Jiang, H. Event-triggered fixed-time integral sliding mode control for nonlinear multi-agent systems with disturbances. *Entropy* **2021**, *23*, 1412. [CrossRef] [PubMed]
14. Young, G.; Scardovi, L.; Leonard, N. Robustness of Noisy Consensus Dynamics with Directed Communication. In Proceedings of the American Control Conference, Baltimore, MD, USA, 30 June–2 July 2010; pp. 6312–6317.
15. Bamieh, B.; Jovanovi, M.R.; Mitra, P.; Patterson, S. Coherence in large-scale networks: Dimension-dependent limitations of local feedback. *IEEE Trans. Autom. Control* **2012**, *57*, 2235–2249. [CrossRef]
16. Patterson, S.; Bamieh, B. Consensus and Coherence in Fractal Networks. *IEEE Trans. Control Netw. Syst.* **2014**, *1*, 338–348. [CrossRef]
17. Patterson, S.; Yi, Y.; Zhang, Z. A Resistance-Distance-Based Approach for Optimal Leader Selection in Noisy Consensus Networks. *IEEE Trans. Control Netw. Syst.* **2018**, *6*, 191–201. [CrossRef]
18. Yi, Y.; Zhang, Z.; Shan, L.; Chen, G. Robustness of First-and Second-Order Consensus Algorithms for a Noisy Scale-Free Small-World Koch Network. *IEEE Trans. Control Syst. Technol.* **2016**, *25*, 342–350. [CrossRef]
19. Sun, W.; Hong, M.; Liu, S.; Fan, K. Leader-follower coherence in noisy ring-trees networks. *Nonlinear Dyn.* **2020**, *102*, 1657–1665. [CrossRef]
20. Liu, J.; Bao, Y.; Zheng, W.; Hayat, S. Network coherence analysis on a family of nested weighted n-polygon networks. *Fractals* **2021**, *29*, 2150260. [CrossRef]
21. Wan, Y.; Namuduri, K.; Akula, S.; Varanasi, M. The impact of multi-group multi-layer network structure on the performance of distributed consensus building strategies. *Int. J. Robust Nonlinear Control* **2012**, *23*, 653–662. [CrossRef]
22. Yang, F.; Jia, Z.; Deng, Y. Eigenvalue Spectrum and Synchronizability of Two Types of Double-Layer Star-Ring Networks with Hybrid Directional Coupling. *Discret. Dyn. Nat. Soc.* **2021**, *2021*, 6623648. [CrossRef]
23. Liao, B.; Lu, Y.; Hu, C.; Feng, L.; Yu, J. Fixed-time output synchronization of multi-layer complex networks under dynamic event-triggering control. *Commun. Nonlinear Sci. Numer. Simul.* **2023**, *127*, 107520. [CrossRef]
24. Xu, M.M.; Lu, J.A.; Zhou, J. Synchronizability and eigenvalues of two-layer star networks. *Acta Phys. Sin.* **2016**, *65*, 028902.
25. Kenyeres, M.; Kenyeres, J. Distributed Mechanism for Detecting Average Consensus with Maximum-Degree Weights in Bipartite Regular Graphs. *Mathematics* **2021**, *9*, 3020. [CrossRef]
26. He, W.; Chen, G.; Han, Q.-L.; Du, W.; Cao, J.; Qian, F. Multiagent Systems on Multilayer Networks: Synchronization Analysis and Network Design. *IEEE Trans. Syst. Man Cybern. Syst.* **2017**, *47*, 1655–1667. [CrossRef]
27. Hu, C.; He, H.; Jiang, H. Edge-Based Adaptive Distributed Method for Synchronization of Intermittently Coupled Spatiotemporal Networks. *IEEE Trans. Autom. Control* **2022**, *67*, 2597–2604. [CrossRef]
28. Hu, C.; He, H.; Jiang, H. Synchronization of complex-valued dynamic networks with intermittently adaptive coupling: A direct error method. *Automatica* **2020**, *112*, 108675. [CrossRef]
29. Kivela, M.; Arenas, A.; Barthelemy, M.; Gleeson, J.P.; Moreno, Y.; Porter, M.A. Multilayer Networks. *J. Complex Netw.* **2014**, *2*, 203. [CrossRef]
30. Wang, Z.; Xia, C.; Chen, Z.; Chen, G. Epidemic Propagation With Positive and Negative Preventive Information in Multiplex Networks. *IEEE Trans. Cybern.* **2021**, *51*, 1454–1462. [CrossRef]
31. Cvetkovic, D.; Rowlinson, P.; Simic, S. *An Introduction to the Theory of Graph Spectra*; Cambridge University Press: New York, NY, USA, 2010.
32. Barik, S.; Pati, S.; Sarma, B. The Spectrum of The Corona of Two Graphs. *SIAM J. Discret. Math.* **2007**, *21*, 47–56. [CrossRef]
33. Zhang, H.; Yang, Y.; Li, C. Kirchhoff index of composite graphs. *Discret. Appl. Math.* **2009**, *157*, 2918–2927. [CrossRef]
34. Liu, Q. The Laplacian spectrum of corona of two graphs. *Kragujev. J. Math.* **2014**, *38*, 163–170. [CrossRef]
35. Wang, X.; Hao, Y.; Wang, Q. On the controllability of Corona product network. *J. Frankl. Inst.* **2020**, *357*, 6228–6240. [CrossRef]
36. Khalifeh, M.H.; Yousefi-Azari, H.; Ashrafi, A.R. The hyper-Wiener index of graph operations. *Comput. Math. Appl.* **2008**, *56*, 1402-1407. [CrossRef]
37. Imrich, W.; Klavzar, S. *Product Graphs*; John Wiley & Sons: New York, NY, USA, 2000.
38. Xu, J.; Yang, C. Connectivity of Cartesian product graphs. *Discret. Math.* **2006**, *306*, 159–165. [CrossRef]
39. Zhang, H.; Yang, Y. Resistance distance and Kirchhoff index in circulant graphs. *Int. J. Quantum Chem.* **2007**, *107*, 330–339. [CrossRef]
40. Yang, Y.; Yu, Y. Resistance Distances and Kirchhoff indices under graph operations. *IEEE Access* **2020**, *8*, 95650–95656. [CrossRef]

41. Liu, Q.; Liu, J.; Cao, J. The Laplacian polynomial and Kirchhoff index of graphs based on R-graphs. *Neurocomputing* **2016**, *177*, 441–446. [CrossRef]
42. Liu, J.; Pan, X. A unified approach to the asymptotic topological indices of various lattices. *Appl. Math. Comput.* **2015**, *270*, 62–73. [CrossRef]